American Journal of Pathology, Vol. 151, No. 1, July 1997

Lymph Vessel Expansion and Function in the Development of Hepatic Fibrosis and Cirrhosis

Brigitte Vollmar, Beate Wolf, Sören Siegmund, Alice D. Katsen, and Michael D. Menger

From the Institute for Clinical and Experimental Surgery, University of Saarland, Homburg/Saar, Germany

The process of lymph vessel expansion and function in the development of CCl_4-induced hepatic fibrosis and cirrhosis was studied using intravital fluorescence microscopy of the rat liver. The unique aspect of our approach was the use of high molecular fluorescein-isothiocyanate-labeled dextran (MW, 150,000) as fluorescent marker, which allowed for simultaneous assessment of both 1) the macromolecular blood hepatocytic exchange from the sinusoidal microvasculature (extra-/intrasinusoidal gray level intensity at 1, 3, 5, and 10 minutes after intravenous injection) and 2) the hepatic lymph system. In animals exposed with CCl_4 up to 4 weeks, macromolecular trans-sinusoidal exchange was found progressively delayed. This was strongly associated with lymph vessel expansion and function, as indicated by a continuous increase of lymph vessel density and area. Delay of macromolecular exchange and lymph vessel expansion was found not further enhanced at fibrotic and cirrhotic stages of 8- and 12-week CCl_4-exposed livers. Linear regression analysis revealed a strong negative correlation between lymphatic network density development and macromolecular trans-sinusoidal exchange ($r^2 = 0.99$; $P < 0.01$). Thus, our study provides for the first time direct evidence for the pivotal role of lymphatic function for macromolecular transport in case of deteriorated sinusoidal hepatocellular exchange capacity. (Am J Pathol 1997, 151:169–175)

During cirrhosis, the hepatic microvascular phenotype is transformed from sinusoids into continuous capillaries. This crucial process includes the excessive deposition of extracellular matrix in the space of Disse with both the formation of basement membranes and the defenestration of endothelial cells, thereby compromising the normal transfer of nutrients between sinusoidal blood and hepatocytes. All metabolites, exchanging between the bloodstream and the hepatocytes, pass through the space of Disse, which extends from the nonluminal side of the sinusoidal endothelial cell to the microvilli of the hepatocellular membrane and which is considered to be confluent with the hepatic lymphatics of the portal tracts.[1,2] Increased lymph flow is known to occur in diffuse abnormalities of liver architecture such as fibrosis and cirrhosis.[3,4] This fluid bypass has supposedly been related to an increase of flow hindrance due to the altered interstitial matrix with lobular distortion[3,5] and, thus, disordered blood hepatocyte exchange capacity.[6] However, there is no report demonstrating direct dependency of trans-sinusoidal hepatocellular exchange and lymphatic drainage.

Herein, we report for the first time the kinetics of hepatic lymph vessel expansion and the functional relation to blood hepatocytic exchange capacity by the unique approach of *in vivo* high resolution fluorescence microscopy in liver fibrotic and cirrhotic rats.

Materials and Methods

Animals and Induction of Liver Fibrosis and Cirrhosis

Male Sprague-Dawley rats (Charles River, Wiga, Sulzfeld, Germany) with a starting weight of ~170 g were given phenobarbital sodium (35 mg/dl) with their drinking water. Three days later the rats were subcutaneously injected with 0.15 ml/100 g body weight

Supported by a grant of the Lucie-Bolte Stiftung (Saarwellingen, Germany) and by a grant of the European Community (BMH 4-CT95-0875).

Accepted for publication March 17, 1997.

Address reprint requests to Dr. Brigitte Vollmar, Institute for Clinical & Experimental Surgery, University of Saarland, D-66421 Homburg/Saar, Germany.

of CCl_4 (Merck, Darmstadt, Germany) in an equal volume of olive oil (Merck, Darmstadt, Germany) twice a week. The duration of treatment included 1 (n = 5), 2 (n = 8), 4 (n = 6), 8 (n = 6), and 12 (n = 7) weeks, respectively. A minimal delay of 3 days after the last dose of CCl_4 was allowed before microcirculation studies were undertaken. Control animals (n = 5), which did not receive phenobarbital or CCl_4 but equal volumes of olive oil, were matched with treated animals based on their body weight. All animals were kept on a standard light cycle and were fed *ad libitum* with a stock pellet dish. Routine histopathology of liver tissue samples (light microscopy, immunohistochemistry (anti-α-smooth muscle actin and anti-desmin), and scanning electron microscopy) confirmed the well known pattern of morphological features of CCl_4-exposed livers.[7–9]

In Vivo *Studies*

The animals were anesthetized with chloral hydrate (36 mg/kg body weight intraperitoneally) and placed in supine position on a heating pad. After tracheotomy, the right carotid artery was exposed and cannulated for heart rate and blood pressure monitoring (PE-50; inner diameter 0.58 mm; Portex, Hythe, UK). An additional catheter (PE-50) in the right jugular vein served as a route for administration of the fluorescent tracer.

After transverse laparotomy, the rats were positioned on their left side and the livers were prepared for intravital fluorescence microscopy by placing the left lobe on a plasticine disk held by an adjustable stage that was attached to the heating pad.[10] Thereby, the lower surface of the liver was situated horizontal to the microscope, which guaranteed adequate homogeneous focus level for the microscopic procedure on the area of liver surface under investigation. In addition, the adjustment of the plasticine disk allowed us to avoid mechanical obstruction of feeding and draining macrovessels and to minimize respiratory movements of the lobe. The exposed area of the left liver lobe was immediately covered with a glass slide to prevent drying of tissue and the influence of ambient oxygen.[10]

Intravital Fluorescence Microscopy and Microcirculatory Analysis

In vivo microscopy was performed using a modified Zeiss Axio-Tech microscope (Zeiss, Oberkochen, Germany) and epi-illumination technique. Microscopic images were registered by a charge-coupled device video camera (FK 6990; Prospective Measurements, San Diego, CA) and were transferred to a video system (VO-5800 PS; Sony, Munich, Germany). Using a 10× objective (10×/0.30, Zeiss) a magnification of ×300 was achieved on the video screen (PVM-1442 QM, with a diagonal of 330 mm; Sony). A solution of 5% fluorescein isothiocyanate (FITC)-labeled dextran (MW, 150,000; 0.1 ml/100 g body weight; Sigma, Deisenhofen, Germany) was injected intravenously (i.v.) as a bolus. By epi-illumination with blue light from a 100-W mercury lamp using a Zeiss filter ((02), 450 to 490-nm/>520-nm excitation/emission wavelength), the appearance of fluorescence in the hepatic microcirculation and its spread into the parenchyma were observed on the video screen and recorded on videotape. For a period of up to 1 hour after the injection of FITC-dextran, the liver parenchyma with individual expansion of lymph vessels was observed.

Trans-sinusoidal exchange was analyzed in three to five sinusoids per observation area (10 to 15 observation areas per animal) by quantifying extravasation of the macromolecular fluorescent marker FITC-dextran 150,000 by means of a computer-assisted image analysis system (CapImage, Zeintl, Heidelberg, Germany) using densitometric techniques.[11,12] Measurements were performed 1, 3, 5, and 10 minutes after i.v. injection of the fluorescent marker. This included densitometric determination of gray levels extra- and intravascularly, ie, within the tissue directly adjacent to the sinusoids (E_1) as well as in the cell-free plasma layer within the sinusoids (E_2).[13] Trans-sinusoidal macromolecular exchange (E) was finally calculated as $E = E_1/E_2$.

Lymph vessels were considered present when perivascular and/or intrahepatic lucencies were present. Lymph vessel expansion was quantitatively assessed by determination of the functional lymphatic density, which was defined as the total length of all lymph vessels per observation area (given as cm/cm^2 (cm^{-1})). To account for variation in lymph vessel size, lymph vessel area was determined planimetrically (given in percentage of the whole observation area). In each observation area, both parameters were assessed by means of a computer-assisted image analysis system (CapImage).

Histopathology

Immunohistochemical staining of liver specimens for demonstration of von Willebrand factor served for differentiation between lymphatic vessels and blood vessels. In brief, paraffinized dewaxed tissue sections (5 μm) were incubated with H_2O_2 to block

endogeneous peroxidase, subsequently pretreated with pronase (2.5 mg/ml) at 37°C for 10 minutes and then incubated with the rabbit polyclonal anti-von-Willebrand-factor primary antibody (Dako, Hamburg, Germany; dilution, 1:200) at 37°C for 90 minutes. As secondary antibody, a biotinylated goat anti-rabbit antibody (Vector Laboratories, Burlingame, CA; dilution, 1:200) was used for streptavidin-biotin complex peroxidase staining (Vectastain ABC peroxidase kits; Camona, Wiesbaden, Germany). 3-Amino-9-ethyl-carbazole was used as chromogen, and the sections were counterstained with hematoxylin.

In addition, liver tissue was excised as rapidly as possible and embedded in OCT compound (Miles, Elkhart, IN) and quickly frozen in liquid nitrogen. The 5- to 8-μm thin sections were cut and collected on poly-L-lysine coated glass slides, air dried, and stored at 4°C until native analysis by fluorescence microscopy (model BX60F, Olympus Optical Co., Tokyo, Japan).

Statistics

All values are means ± SEM. After proving the assumption of normality and homogeneity of variance across groups, differences between groups were calculated using the unpaired Student's *t*-test. Differences were considered significant for $P < 0.05$. To assess the correlation between functional lymphatic density and trans-sinusoidal macromolecular exchange, linear regression analysis was performed (SigmaStat, Jandel Corp. San Rafael, CA).

Results

Intravital Microscopic Findings

Trans-sinusoidal macromolecular exchange, ie, the ratio of extra- to intravascular gray level intensities, of untreated control animals was 0.87 ± 0.02 at 1 minute and slightly increased to 0.93 ± 0.02 at 10 minutes after i.v. injection of FITC-dextran (Figure 1). In animals treated with CCl_4 for 1, 2, and 4 weeks, trans-sinusoidal macromolecular exchange was found progressively delayed with 1-minute values of 0.85 ± 0.01, 0.81 ± 0.04, and 0.74 ± 0.03 ($P < 0.05$ *versus* controls). At 10 minutes after i.v. injection of FITC-dextran, however, the ratio of extra- to intravascular gray level intensities of 0.95 ± 0.03, 0.95 ± 0.03, and 1.04 ± 0.05 were in the range of those of untreated control animals, indicating, with the exception of the delay, a still comparable overall capacity of trans-sinusoidal macromolecular exchange (Figure 1). With increasing duration of CCl_4 exposure for

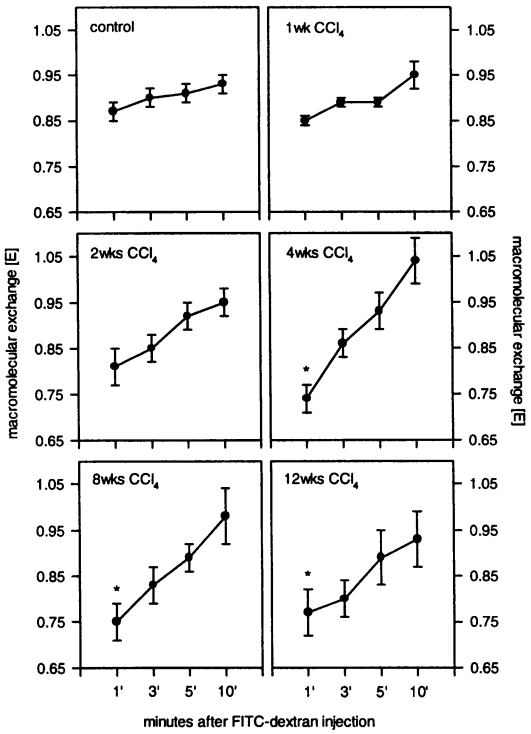

Figure 1. *Trans-sinusoidal macromolecular exchange (E), ie, ratio of extra- to intrasinusoidal gray level intensities at 1, 3, 5, and 10 minutes after i.v. injection of high molecular FITC-dextran (MW, 150,000) in livers of animals after CCl_4 exposure for 1 (n = 5), 2 (n = 8), 4 (n = 6), 8 (n = 6), and 12 weeks (n = 7). Untreated animals served as controls (n = 5). Measurements were performed using intravital fluorescence epi-illumination microscopy and densitometric techniques for off-line analysis. Means ± SEM;* *P < 0.05 versus controls.

8 and 12 weeks, pattern of trans-sinusoidal macromolecular exchange did not further change with delayed values of 0.75 ± 0.04 and 0.77 ± 0.05 at 1 minute ($P < 0.05$ *versus* controls) as well as normal values with 0.98 ± 0.06 and 0.93 ± 0.06 at 10 minutes after i.v. injection of FITC-dextran (Figure 1).

Assessment of the formation of hepatic lymphatics during the time course of liver fibrosis and cirrhosis revealed a progressive increase of functional lymphatic density (Figure 2, A–D) with a mean value of 12.3 ± 8.0, 19.9 ± 10.4, and 49.8 ± 9.0 cm^{-1} after 1, 2, and 4 weeks of CCl_4 exposure, respectively ($P < 0.01$ *versus* controls; Figure 3A). At the stage of CCl_4 exposure for 8 and 12 weeks, functional lymphatic density was found unchanged, presenting with values of 44.4 ± 5.7 and 38.2 ± 2.6 cm^{-1} ($P <$ 0.01 *versus* controls; Figure 3A). In parallel with the values of functional lymphatic density, the area of lymphatic vessels progressively increased (Figure 2, A–D) from 2.6 ± 1.7% to 6.5 ± 3.4 and 14.5 ± 1.7% after 1, 2, and 4 weeks of CCl_4 exposure with no further change after CCl_4 exposure for 8 (13.2 ± 2.1%) and 12 (11.6 ± 0.7%) weeks ($P < 0.01$ *versus*

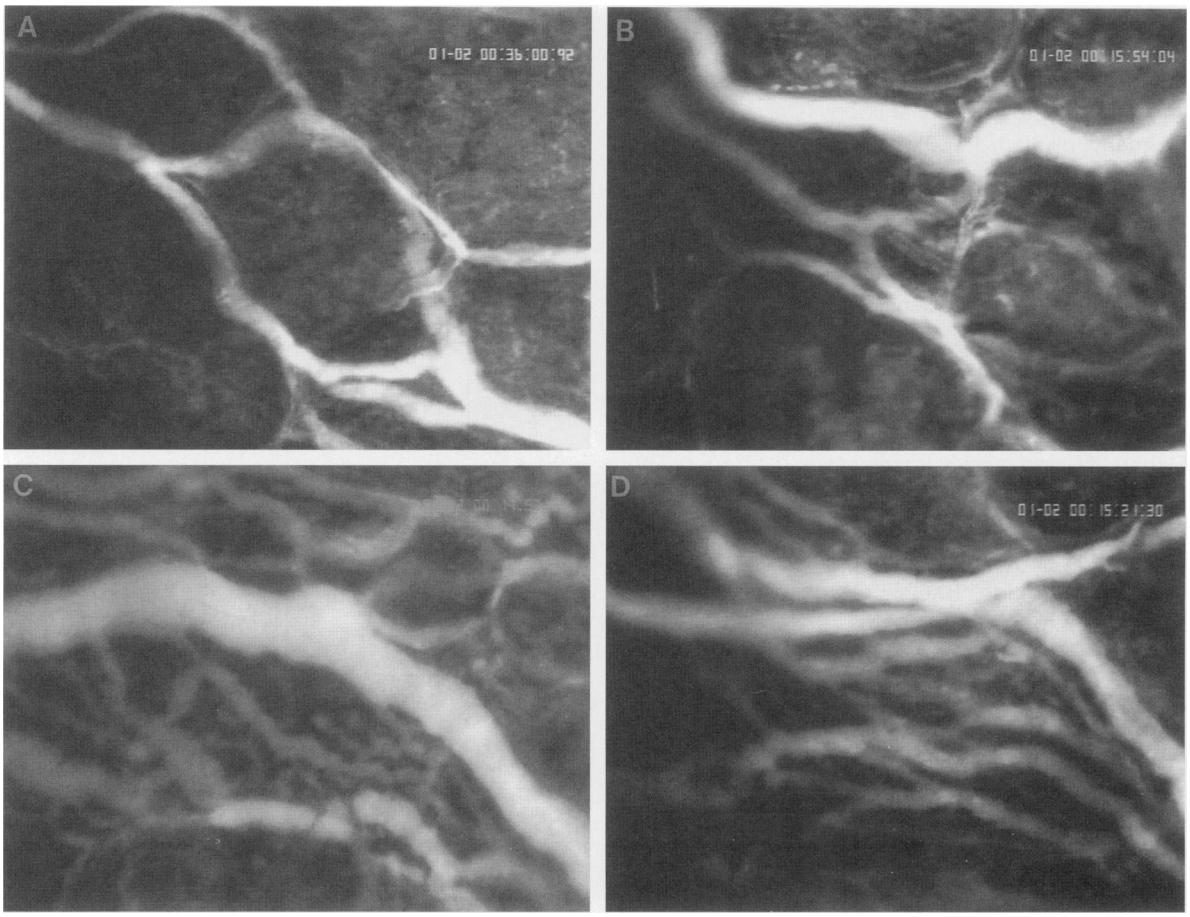

Figure 2. *Intravital fluorescence microscopic image of the lymphatic network of the liver after CCl_4 exposure for 1* (**A**), *2* (**B**), *4* (**C**), *and 12* (**D**) *weeks. During initial stages of CCl_4 exposure (1, 2, and 4 weeks;* **A** *to* **C**), *lymph vessel density was found progressively increased with no further change in 8- and 12-week-exposed livers* (**D**). *Fluorescence epi-illumination technique after i.v. injection of high molecular weight FITC-labeled dextran (MW, 150,000) as fluorescent marker; magnification, ×100.*

controls; Figure 3B). In untreated control animals, no lymphatic transport of FITC-dextran was visualized (Figure 3, A and B).

Linear regression analysis between functional lymphatic density and transsinusoidal macromolecular exchange at 1 min after FITC-dextran injection revealed a significant ($P < 0.01$) correlation with $r^2 = 0.99$ (Figure 4).

Histological Findings

Immunohistochemical analysis for von Willebrand factor revealed a marked staining of endothelial cells lining post-sinusoidal venules as well as hepatic arterial and, in particular, portal venous vessels and, thus, allowed to separate lymphatics within the portal tracts, which do not or at least only weakly stain for von Willebrand factor (Figure 5, A and B). Additional indication for lymphatics was given by the intraluminal absence of blood cells. Whereas in normal hepatic tissue, lymphatics were rarely observed and, then, bile duct and hepatic arteriole were in most instances larger than the lymphatic duct (Figure 5A), lymphatics were constantly observed in tissue sections of CCl_4-induced liver fibrotic and cirrhotic animals, exhibiting engorgement with diameters at least as large as that of the adjoining arterioles and bile ducts (Figure 5B). Beside their location within the portal tracts, fluorescence microscopy of cryostat sections revealed FITC-conducting lymph vessels in the fibrous septa of liver tissue after repetitive CCl_4 exposure (Figure 6).

Discussion

Although increased lymph production in human cirrhosis was repeatedly described and dilated lymph vessels were documented by angiography and computer tomographic scans in liver fibrotic and cirrhotic patients,[14,15] no reports of *in vivo* studies exist specifically designed to determine the expansion and

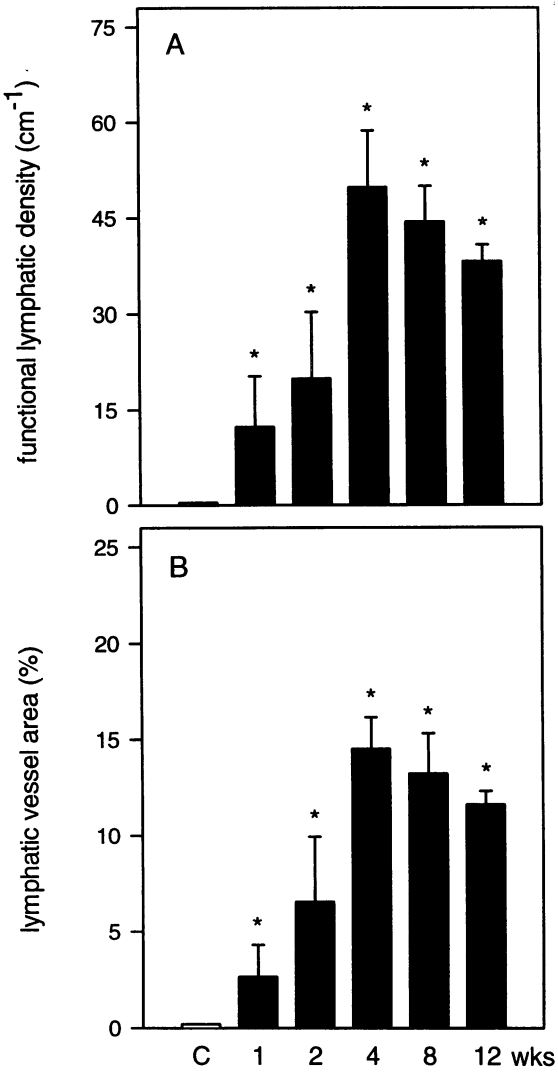

Figure 3. *Functional lymphatic density, ie, length of lymphatic vessels per area, in cm/cm^2* (A) *and lymphatic vessel area, in percent* (B), *in livers of animals after CCl_4 exposure for 1 (n = 5), 2 (n = 8), 4 (n = 6), 8 (n = 6), and 12 (n = 7) weeks. Untreated animals served as controls* (C; *n = 5*). *Measurements were performed using intravital fluorescence epi-illumination microscopy and a computer-assisted image analysis system for off-line analysis. Means ± SEM;* *P < *0.01* versus *controls.*

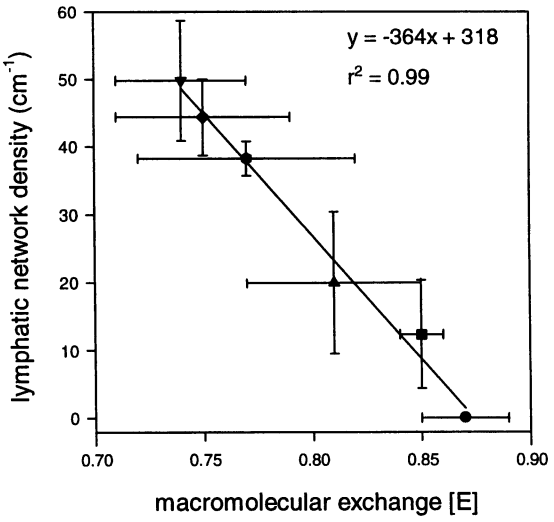

Figure 4. *Regression analysis between functional lymphatic network density (cm^{-1}) and macromolecular exchange of FITC-dextran 150,000 at 1 minute after i.v. injection of the fluorescent marker.* ●, *control livers;* ■, *livers after 1 week of CCl_4 exposure;* ▲, *livers after 2 weeks of CCl_4 exposure;* ▼, *livers after 4 weeks of CCl_4 exposure;* ◆, *livers after 8 weeks of CCl_4 exposure;* ●, *livers after 12 weeks of CCl_4 exposure.*

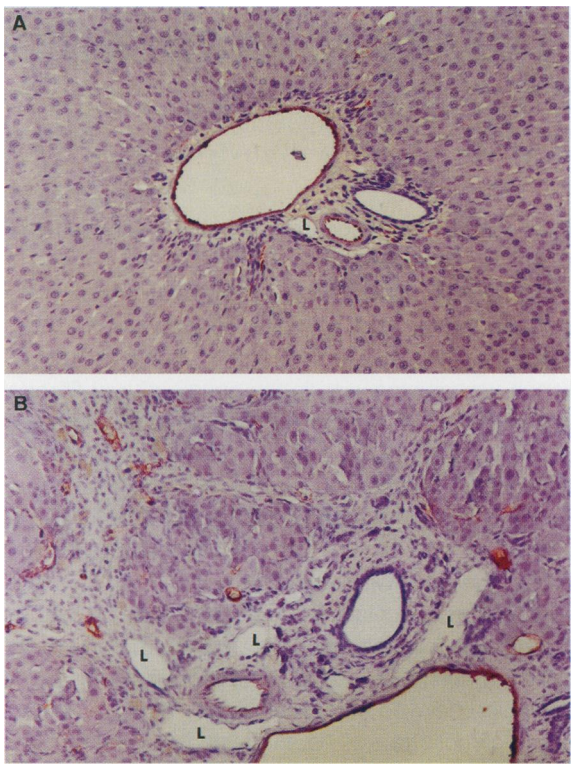

Figure 5. *Immunohistochemical staining of normal liver tissue* (A) *and liver tissue after 8 weeks of CCl_4 exposure* (B) *with an antibody directed against von Willebrand factor.* A: *Endothelial cells of postsinusoidal venules as well as hepatic arterioles and portal venules within the portal tracts show an intense reaction, whereas staining of the endothelium for von Willebrand factor is lacking in the lymphatic vessel (L).* B: *Engorged hepatic lymph vessels (L) within the portal tracts of liver cirrhotic tissue with still absent staining for von Willebrand factor. Note the intense staining of the vessels within the perinodular fibrotic tissue and along hepatic sinusoids in cirrhotic nodules. Magnification, ×220.*

function of lymphatics in the time course of development of liver fibrosis and cirrhosis. Using high-resolution fluorescence microscopy, the present study shows that the initial stages after CCl_4 exposure of rats (1 to 4 weeks) were characterized by a progressive delay in macromolecular blood hepatocytic exchange, implying the appearance of diffusion barriers within the fibrotic and cirrhotic liver. In parallel, in these animals, marked increases of both lymph vessel density and lymph vessel area were observed. Linear regression analysis revealed a significant correlation in that the more delayed the trans-sinusoidal

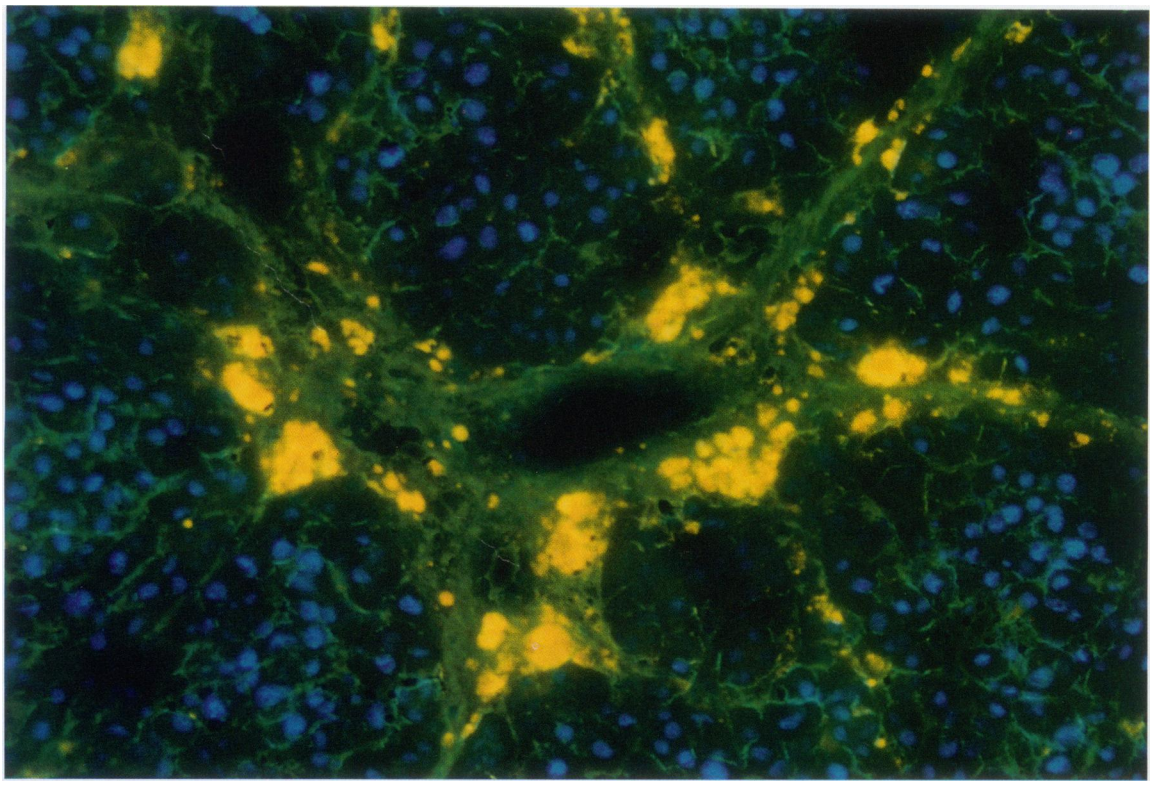

Figure 6. *Fluorescence microscopic analysis (triple exposure: 330 to 390/>430-nm, 450 to 490/>515-nm, and 530 to 560/>580-nm excitation/emission wavelength) of cryostat sections of liver tissue after 4 weeks of CCl_4 exposure. Note the numerous FITC-dextran conducting lymph vessels (green fluorescence) within the autofluorescent fibrous septa of liver fibrotic tissue (yellow fluorescence). Parenchymal cells (blue fluorescence) were stained* in vivo *by Bisbenzamide H33342 (20 μmol/kg i.v.). Magnification, ×220.*

macromolecular exchange capacity, the higher lymphatic network density.

The unique aspects of our *in vivo* fluorescence microscopic approach, employed in the present study, includes 1) the assessment of the kinetics of hepatic lymph vessel expansion in the course of liver fibrosis and cirrhosis with quantitative analysis of development of functional lymphatic network density and 2) the determination of trans-sinusoidal macromolecular exchange capacity of FITC-dextran 150,000, which serves as an indirect marker for blood hepatocytic barrier function. Within the first weeks of CCl_4 exposure, macromolecular exchange of FITC-dextran within the hepatic microcirculation was found progressively delayed, which goes along with previous studies demonstrating delayed plasma clearance of different tracers in cirrhotic rats.[16] As suggested by others,[16] the appearance of diffusion barriers might reduce the trans-sinusoidal hepatocellular exchange capacity, which may finally lead to an unavailability of blood solutes, such as FITC-dextran, to hepatocytes. The significant point of the present study is the association of the delay of macromolecular blood hepatocytic exchange with an increase of lymphatic drainage, thereby carrying abundant FITC-dextran. In livers of untreated control animals, no lymphatic transport of FITC-dextran can be observed, as FITC-dextran is freely diffusible, as indicated by the rapid trans-sinusoidal exchange, and completely taken up by hepatocytes. So far, lymphatics of the liver have been recognized to play an important role in overall regulation of body fluid balance[1,17] and, in cases of liver cirrhosis, increased lymph flow[18] has repeatedly been suggested as an important mechanism for fluid to bypass increased sinusoidal/post-sinusoidal resistance.[3,19] Our study provides substantial *in vivo* evidence that lymphatic drainage functions as a compensatory mechanism, guaranteeing the transport of macromolecules (ie, FITC-dextran), which are, although delayed, effectively removed from the circulation but trapped extravascularly due to diffusion-barrier-induced hindrance of hepatocellular uptake.

In conclusion, the present study presents both the first documentation and the quantitative characterization of the relation between compensatory lymph vessel expansion and altered blood hepatocytic exchange. This link is now known to include the function of macromolecular lymphatic transport linearly dependent on the deterioration of trans-sinusoidal hepatocytic exchange capacity.

References

1. Lautt WW, Greenway CV: Conceptual review of the hepatic vascular bed. Hepatology 1987, 7:952–963
2. Hardonk MJ, Atmosoerodjo-Briggs J: Evidence for the anatomical connection between the space of Disse and the portal tract in human and rat liver. Cells of the Hepatic Sinusoid, Vol 4. Edited by DL Knook, E Wisse. Leiden, The Netherlands, Kupffer Cell Foundation, 1993, pp 182–184
3. Ludwig J, Linhart P, Baggenstoss AH: Hepatic lymph drainage in cirrhosis and congestive heart failure. Arch Pathol 1968, 86:551–562
4. Witte MH, Dumont AE, Cole WR, Witte CL, Kinter K: Lymph circulation in hepatic cirrhosis. Ann Intern Med 1969, 70:303-310
5. Shimada Y: Observations on hepatic superficial lymph flow. Lymphology 1979, 12:11–13
6. Witte CL, Witte MH, Dumont AE: Lymph imbalance in the genesis and perpetuation of the ascites syndrome in hepatic cirrhosis. Gastroenterology 1980, 78:1059–1068
7. Proctor E, Chatamra K: High yield micronodular cirrhosis in rats. Gastroenterology 1982, 83:1183–1190
8. Tsukamoto H, Matsuoka M, French SW: Experimental models of hepatic fibrosis: a review. Semin Liver Dis 1990, 10:56–65
9. Martinez-Herandez A: The hepatic extracellular matrix. II. Electron immunohistochemical studies in rats with CCl_4-induced cirrhosis. Lab Invest 1985, 53:166–186
10. Vollmar B, Glasz J, Leiderer R, Post S, Menger MD: Hepatic microcirculatory perfusion failure is a determinant for liver dysfunction in warm ischemia-reperfusion. Am J Pathol 1994, 145:1421–1431
11. Hultström D, Svensjö E: Simultaneous fluorescence and electron microscopical detection of bradykinin induced macromolecular leakage. Bibl Anat 1977, 15: 466–468
12. Pries AR: A versatile video image analysis system for microcirculatory research. Int J Microcirc Clin Exp 1988, 7:327–345
13. Menger MD, Pelikan S, Steiner D, Messmer K: Microvascular ischemia-reperfusion injury in striated muscle: significance of "reflow-paradox." Am J Physiol 1992, 263:H1901–H1906
14. Sadek AM, Ismail AM, Enein AA, Hassanein E, Massoud OG, El-Assi MH: Percutaneous trans-hepatic lymphography: evaluation in schistosomal hepatic fibrosis. Lymphology 1976, 9:47–52
15. Aspestrand F, Schrumpf E, Jacobsen M, Hanssen L, Endresen K: Increased lymphatic flow from the liver in different intra- and extrahepatic diseases demonstrated by CT. J Comput Assist Tomogr 1991, 15:550–554
16. Martinez-Hernandez A, Martinez J: The role of capillarization in hepatic failure: studies in carbon tetrachloride-induced cirrhosis. Hepatology 1991, 14:864–874
17. Laine GA, Hall JT, Laine SH, Granger HJ: Transsinusoidal fluid dynamics in canine liver during venous hypertension. Circ Res 1979, 45:317–323
18. Huth F, Wilde A, Schulten HJ, Berger S: Morphological studies on pathophysiology of the liver lymph vessel system. Virch Arch A Pathol Anat Histopathol, 1970, 351:41–67
19. Dumont AE, Mulholland JH: Flow rate and composition of thoracic duct lymph in patients with cirrhosis. N Engl J Med 1960, 263:471–474